

Nonlinear volatility of river flux fluctuationsValerie N. Livina,¹ Yosef Ashkenazy,² Peter Braun,³ Roberto Monetti,⁴ Armin Bunde,⁵ and Shlomo Havlin¹¹*Minerva Center and Department of Physics, Bar-Ilan University, Ramat-Gan 52900, Israel*²*Department of Earth, Atmospheric and Planetary Sciences, Massachusetts Institute of Technology, Cambridge, Massachusetts 02139*³*Bayerisches Landesamt für Wasserwirtschaft, Lazarettstrasse 67, D-80636 München, Germany*⁴*Center for Interdisciplinary Plasma Science (CIPS), Max-Planck-Institut für Extraterrestrische Physik, Giessenbachstrasse 1, 85749 Garching, Germany*⁵*Institut für Theoretische Physik III, Justus-Liebig-Universität Giessen, Heinrich-Buff-Ring 16, 35392 Giessen, Germany*

(Received 25 September 2002; revised manuscript received 12 November 2002; published 7 April 2003)

We study the spectral properties of the magnitudes of daily river flux increments, the volatility. The volatility series exhibits (i) strong seasonal periodicity and (ii) power-law correlations for time scales less than 1 yr. We test the nonlinear properties of the river flux increment series by randomizing its Fourier phases and find that the surrogate volatility series (i) has almost no seasonal periodicity and (ii) is weakly correlated for time scales less than 1 yr. We quantify the degree of nonlinearity by measuring (i) the amplitude of the power spectrum at the seasonal peak and (ii) the correlation power-law exponent of the volatility series.

DOI: 10.1103/PhysRevE.67.042101

PACS number(s): 05.40.–a, 92.70.Gt, 92.40.Cy

Climate is strongly forced by the periodic variations of the Earth with respect to state of the solar system. The seasonal variations in the solar radiation cause periodic changes in temperature and precipitation, which eventually lead to seasonal periodicity of river flow. In spite of this well-defined seasonal change, river flow exhibits highly unpredictable complex behavior; floods and droughts are usually unexpected and cause severe damage in life, housing, and agriculture products. Hence, river flow is likely to have an indirect nonlinear response to the various forcings, among them the seasonal changes in solar radiation.

Many components of the water budget of a catchment are coupled in a nonlinear fashion. The key for all interactions between atmospheric processes like precipitation, temperature, humidity, and surface runoff is the soil. The dynamic state of this key variable is highly nonlinear. An essential feature in this respect is, e.g., the dependence of this dynamics from the past.

By means of the methods proposed here, it will be possible to characterize quantitatively the degree of nonlinearity of the involved processes in a compact way by investigating the outputs of the catchment (the resulting runoff time series) only. This check would be very helpful, for example, in view of the design of time series models or statistical prediction algorithms.

There are several statistical approaches to the study of river flow fluctuations. For instance, river flow fluctuations have broad probability distribution, i.e., the tails of the distribution decay approximately as a power law [1,2]. Moreover, river flow fluctuations have unique temporal organization; they are long-range power-law correlated and possess scale invariant structure [3]. These power-law correlations are usually characterized by scaling exponents [4,5] as was originally defined by Hurst for the Nile River floodings [6]. Similar power-law correlations occur also for temperature fluctuations in the atmosphere [7] and in the oceans. However, such scaling laws only quantify the linear properties (two-point correlations) of a time series. Here we study other nonlinear aspects of river flow fluctuations.

A nonlinearity of a stationary time series may be defined with respect to its Fourier phases [8,9]. The series where its statistical properties are independent of the Fourier phases is *linear*, otherwise the series is *nonlinear*. For instance, autoregression processes and fractional Brownian motion are linear, while multifractal processes are nonlinear. Recently, it has been shown that volatility correlations of long-range power-law correlated time series reflect the degree of nonlinearity of a time series [9]. Given a time series x_i , the volatility series is defined as the magnitudes of the series increments, $|\Delta x_i| \equiv |x_{i+1} - x_i|$. It was found that long-range correlated linear series have uncorrelated volatility series, while long-range correlated nonlinear series have correlated volatility series; see Ref. [9] for details. Power-law correlations in the volatility series indicate that the magnitudes $|\Delta x_i|$ are clustered into patches of small and big magnitudes—a big magnitude increment is likely to precede a big magnitude increment, and vice versa. When the volatility series $|\Delta x_i|$ is uncorrelated, the increment series is homogeneous. Volatility correlations were found, e.g., in econometric time series [10], heartbeat interval series [9,11], and human interstride interval series [12].

Here we study the volatility properties of daily river flow fluctuations. We first extend the notion of volatility to periodic time series. We find that after randomizing the Fourier phases of the river flow increment series, the periodicity of the volatility series is almost diminished, indicating that “periodic volatility” is a result of nonlinearity. We also find long-range volatility correlations for time scales below 1 yr. Our results suggest that clusters of magnitudes of river flow increments appear in two ways: periodically and in long-range correlated manner.

We analyze the daily river flux time series of 30 rivers scattered around the globe. The mean flux of these rivers ranges from $\sim 0.6 \text{ m}^3/\text{s}$ to $\sim 2 \times 10^5 \text{ m}^3/\text{s}$, covering more than five orders of magnitudes. The series length ranges from 26 yr to 171 yr, with an average length of 81 yr. Figure 1 shows a typical example of 4 yr (1986–1990) of River flow

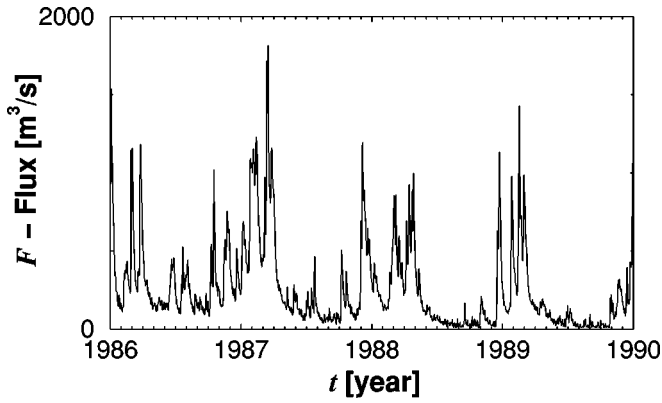


FIG. 1. Typical river flow time series of the Maas River (Europe). The record shows a periodic pattern with irregular fluctuations. Fluctuations are large around large river flow and small around small river flow.

data (Maas river, Europe). It is evident that fluctuations around large river flows are large, while fluctuations around small river flows are small.

To study the nonlinear properties of the river flow record, we apply a surrogate data test to the river flow increment series. Shortly, the surrogate series is created as follows: (i) shuffle the original series, (ii) Fourier transform the shuffled series and adjust its power spectrum to the power spectrum of the original series, and (iii) inverse transform the series from (ii) and adjust its histogram to the histogram of the original series. Repeat steps (ii) and (iii) till convergence; for more details, see Ref. [8]. The surrogate data test preserves both the power spectrum and the probability distribution of the river flow increment series but randomizes the Fourier phases. Thus, the surrogate data test linearizes the series under consideration. Since the histograms of the original incre-

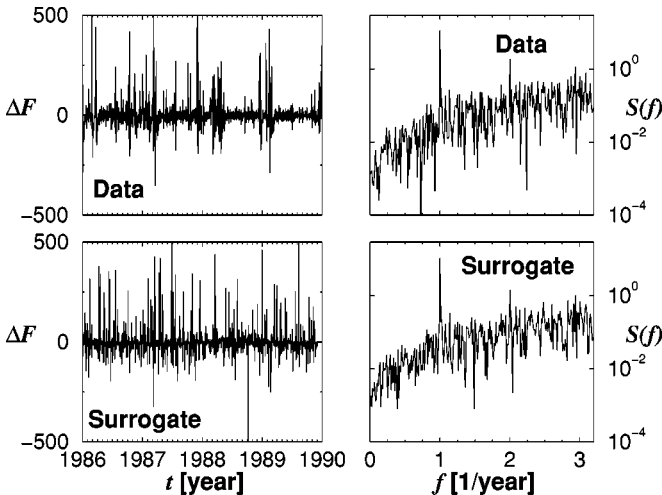


FIG. 2. River flux increment series of the Maas River (left panels) and their corresponding power spectra (right panels) before (upper panels) and after (lower panels) the surrogate test for nonlinearity. The series length is 80 yr where just the last 4 yr data are shown (in the left panels). The original river flow increment series and the surrogate increment series have identical probability distributions and very similar power spectra.

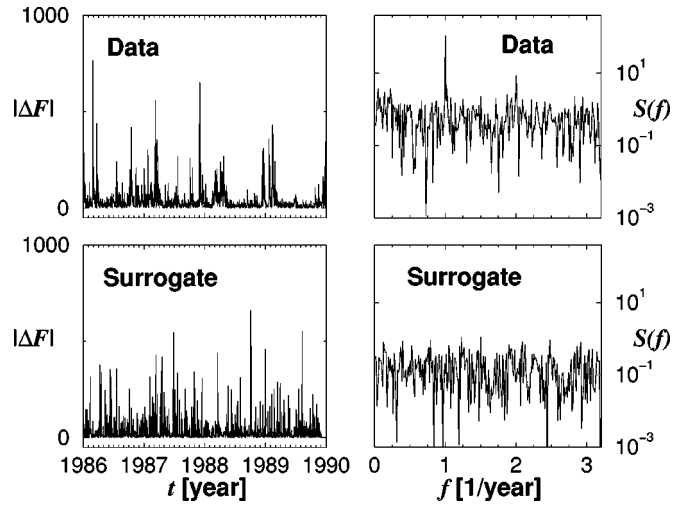


FIG. 3. Same as Fig. 2, but for the river flow volatility series $|\Delta F_i| \equiv |F_{i+1} - F_i|$. Here, the original volatility series shows a pronounced seasonal peak, while the surrogate volatility series does not show such a peak, indicating that the periodicity in the volatility series is a result of nonlinearity.

ment series and of the surrogate series are identical, one can be sure that the probability distribution is not the source of the nonlinearity of the data. Figure 2 shows the river flow increment series and its power spectrum before and after the surrogate data test. Although the river flow increment series exhibits irregular behavior, its power spectrum shows a very pronounced seasonal peak with few harmonics. As expected, the surrogate series shows a similar pattern with very similar power spectrum.

Next we compare the power spectrum of the volatility series obtained from the original increment river flow series with the surrogate series (Fig. 3). The power spectrum of the original volatility series shows a pronounced seasonal peak, while the power spectrum of the surrogate volatility series has no seasonal periodicity. The seasonal periodicity of the original volatility series may be associated with the increased

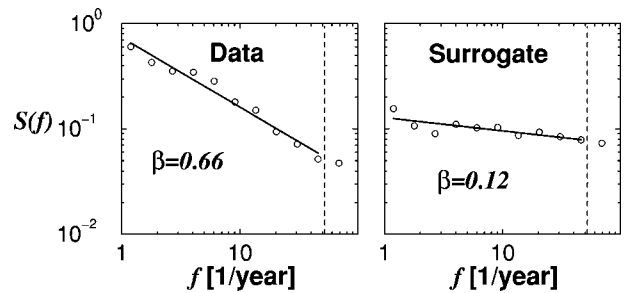


FIG. 4. Log-log plot of the power spectra shown in Fig. 3. The solid lines are the best fits of $S(f) \sim 1/f^\beta$ for frequencies $1.05 \text{ yr}^{-1} < f < 52 \text{ yr}^{-1}$. The original volatility series (left panel) decays as a power law ($1/f^{\beta=0.66}$), indicating long-range correlations. The power spectrum of the linearized surrogate volatility (right panel) series has a flatter spectrum, indicating much less correlated behavior. Thus, correlations in the volatility series are an additional measure for nonlinearity of the river flow increment time series.

fluctuation for large river flux (Fig. 1). The absence of seasonal periodicity for the surrogate volatility series is somehow counterintuitive since the surrogate series itself is as periodic as the original river flow increment series, while a simple inversion operation of the negative values of Δx_i to obtain $|\Delta x_i|$ diminishes this periodicity. This absence of the seasonal periodicity from the surrogate volatility series indicates that periodicity in the magnitude series is a result of nonlinearity associated with correlations in the Fourier phases. We suggest that the amplitude of the seasonal peak of the original volatility series compared to the seasonal peak of the surrogate volatility series can quantify the degree of nonlinearity.

We use the power spectra of the original and surrogate volatility series to analyze the correlation properties of these series. A series x_i is long-range correlated if its autocorrelation function decays as a power law, $C(l) = [1/(N-l)] \sum_{i=1}^{N-l} x_{i+l} x_i \sim l^{-\gamma}$, where N is the series total length, l is the lag, and γ is the correlation exponent ($0 < \gamma < 1$). Then also the power spectrum follows the scaling law $S(f) \sim 1/f^\beta$, where $\gamma = 1 - \beta$. In Fig. 4 we show the power spectra of the original and surrogate volatility series for frequencies larger than 1 yr^{-1} . While the power spectrum of the

surrogate volatility series is almost flat, the power spectrum of the original volatility series decays as a power law with an exponent of $\beta \approx 0.66$. Thus (i) the original volatility series is power-law correlated and (ii) its correlations are a nonlinear measure since they significantly reduced after the surrogate data test. The interpretation of these correlations is that there are clusters of big magnitudes $|\Delta F_i|$ that are statistically followed by patches of big magnitudes. These clusters are in addition to the periodic clustering (shown in Fig. 3). We also repeated the scaling analysis with a more advanced method, the detrended fluctuation analysis [13], and find less noisy but similar results [14].

We summarize the periodic volatility and the long-range volatility correlation results for 30 rivers in Fig. 5. To systematically compare the seasonal periodicity of different rivers, we first normalize the volatility series by subtracting its mean and dividing it by its standard deviation; thus, the area under the power spectrum of the different volatility series should be the same. The seasonal peak of the volatility series exists for all 30 rivers, and is significantly higher than the seasonal peak of the surrogate volatility series (Fig. 5, upper panel). The scaling exponent β of the original volatility series (Fig. 5, lower panel) indicates correlations; in most of the cases (27/30=90%) the exponent of the original volatility series lies above 1 standard deviation of the exponent of the surrogate volatility series. The average ± 1 standard deviation of the scaling exponent of original volatility series is $\beta = 0.49 \pm 0.11$, and is significantly higher than the average ± 1 standard deviation of the scaling exponent of the surrogate volatility series $\beta = 0.18 \pm 0.13$. The p value of the student's t test is less than 10^{-6} . For time scales above 1 yr, the volatility series is only weakly correlated with average exponent $\beta = 0.27 \pm 0.26$.

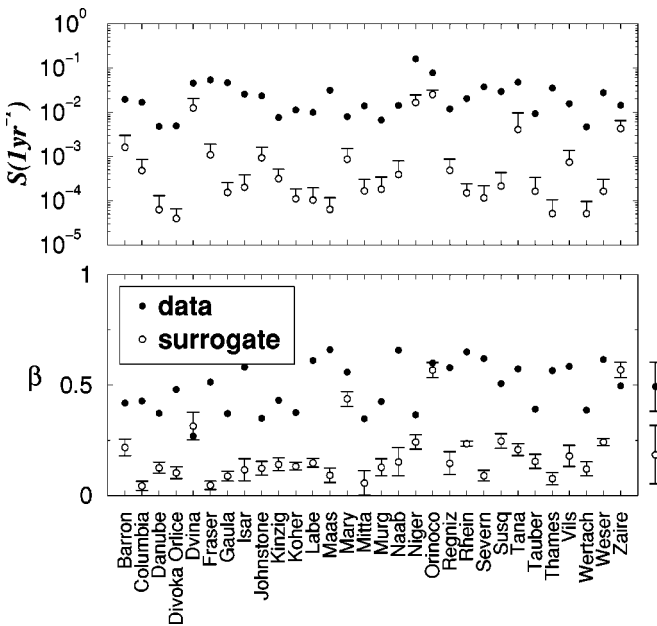


FIG. 5. A summary of the results obtained for 30 rivers around the world. For each river flow increment series (●), we generated ten surrogate series (○), and calculated the amplitude of the seasonal peak of the volatility series (upper panel) and the scaling exponent β for frequencies $1.05 \text{ yr}^{-1} < f < 52 \text{ yr}^{-1}$ (lower panel); the average and 1 standard deviation are shown. In order to systematically compare the results of the different rivers, we subtract from the volatility series its mean and normalize it by its standard deviation. The seasonal peak of the volatility series is significantly higher compared to the seasonal frequency of the surrogate volatility series (upper panel). The scaling exponent β shown in the lower panel is systematically higher for the original volatility series. For 27 rivers, the original volatility exponent lies well above the surrogate series exponent. The error bars on the right hand side are the group average ± 1 standard deviation.

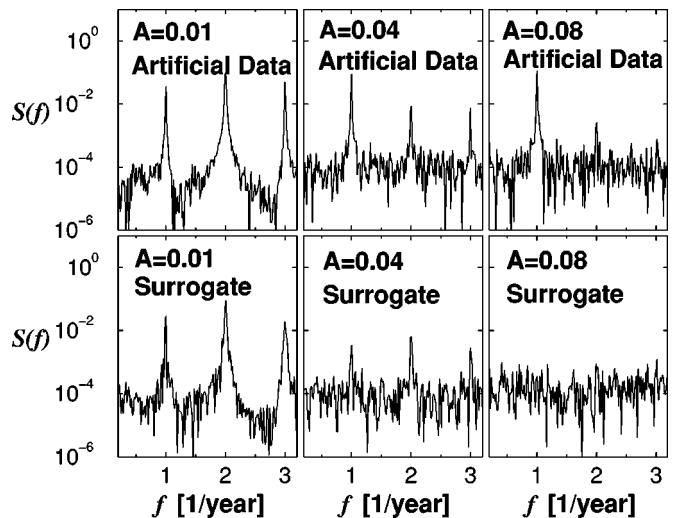


FIG. 6. The power spectrum of the normalized volatility series $|\Delta x_i|$ of an artificial series $x_i = (1 + A \eta_i) s_i$ for different noise levels A ; see text. The power spectra of the original (upper panels) and surrogate (lower panel) volatility series are shown. When the noise level increases (from left to right), the seasonal peak of the surrogate volatility series reduces. The harmonics of the power spectra are partly caused by the asymmetric x_i and partly because of the absolute value operation for the volatility series.

Thus, we find two measures of nonlinearity related to the river flow data, periodic volatility and long-range correlated volatility. These two measures are related to the clustering of the magnitudes of river flow fluctuations, periodic and long-range correlated clustering.

To study in more detail the possible source for such a seasonal periodicity of the volatility series, we propose a simple scheme to generate series with some similar characteristics as for the river flow data. To mimic the enhanced fluctuations for large river flow, we assume that $x_i = (1 + A\eta_i)s_i$, where η_i is a Gaussian white noise (zero mean and unit standard deviation), A is the noise level, and s_i is an asymmetric periodic function,

$$s_i = s_{j+nT} = \begin{cases} 1 + \cos(2\pi f j) & \text{for } 0 \leq j < \frac{2}{3}T, \\ 1 - \cos(4\pi f j) & \text{for } \frac{2}{3}T \leq j < T, \end{cases} \quad (1)$$

where $T=365$ is the time period in arbitrary units, j is an integer $0 \leq j < T$, $f=0.75/T$, and n is an integer. x_i decreases for $2/3$ of the time period T and increases for $1/3$ of this time period. When the noise level A increases, the nonlinear term $A\eta_i s_i$ also increases. We generate x_i series with different noise levels, and then calculate the power spectrum of the normalized volatility series $|\Delta x_i|$ of the original and surrogate Δx_i series (Fig. 6). We find that when the noise level is relatively small the seasonal peak is present in both the original and surrogate volatility series. The periodicity of the surrogate volatility series diminishes for increasing noise level. Thus, the larger is the difference between the peak of original

volatility series and the peak of the surrogate volatility series, the larger is the nonlinearity of Δx_i . This scheme indicates that the surrogate data test does not always diminish the seasonal periodicity of the volatility series, but rather eliminates the nonlinear part of the process which is proportional to the noise level. We also analyzed time series generated by a realistic hydrological model (ASGi model for Bavaria, Germany [15]) for the Naab, Regniz, and Vils Rivers. Both the seasonal periodicity of the volatility series and its correlations are reproduced by the model and disappear after phase randomization, as for the real data.

In summary, we have analyzed the periodic and long-range correlated volatility of river flow data for 30 rivers around the globe. We find that the volatility series are correlated with a power-law behavior for time scales less than 1 yr. The periodic volatility and the long-range correlated volatility disappear after randomizing the Fourier phases; indicating that these volatility features result from a nonlinear dynamical process. These volatility features may quantify the degree of nonlinearity. We suggest that such nonlinear features may result from an interaction between noise and the seasonal trends.

Preliminary analysis of other climate records, such as daily temperature and pressure records, shows the existence of periodic and long-range volatility with similar properties as for the river flow data. Thus, the results presented here may be generic for other climate records.

We gratefully acknowledge financial support from the Israel Science Foundations and the Deutsche Forschungsgemeinschaft. Y.A. thanks the BIKURA Foundation for financial support.

-
- [1] R.U. Muddock and J.S. Gulliver, *J. Water Resour. Plan. Manage.* **119**, 473 (1993).
 [2] C.N. Kroll and R.M. Vogel, *J. Hydrologic Eng.* **7**, 137 (2002).
 [3] D.L. Turcotte and L. Greene, *Stochastic Hydrol. Hydr.* **7**, 33 (1993).
 [4] Y. Tessier *et al.*, *J. Geophys. Res., [Atmos.]* **101**, 26 427 (1996).
 [5] G. Pandey, S. Lovejoy, and D. Schertzer, *J. Hydrol.* **208**, 62 (1998).
 [6] H.E. Hurst, *Trans. Am. Soc. Civ. Eng.* **116**, 770 (1951).
 [7] E. Koscielny-Bunde, A. Bunde, S. Halvin, H.E. Roman, Y. Goldreich, and H.J. Schnellhuber, *Phys. Rev. Lett.* **81**, 729 (1998); R.A. Monetti, S. Halvin, and A. Bunde, *Physica A* (to be published).
 [8] T. Schreiber and A. Schmitz, *Physica D* **142**, 346 (2000).
 [9] Y. Ashkenazy, P.Ch. Ivanov, S. Havlin, Ch.K. Peng, A.L. Goldberger, and H.E. Stanley, *Phys. Rev. Lett.* **86**, 1900 (2001); Y. Ashkenazy S. Havlin, P.Ch. Ivanov, Ch.-K. Peng, V. Shulte-Frohlinde, and H.E. Stanley, *Physica A* (to be published), e-print cond-mat/0111396.
 [10] Y.H. Liu, P. Gopikrishnan, P. Cizeau, M. Meyer, C.-K. Peng, and H.E. Stanley, *Phys. Rev. E* **60**, 1390 (1999).
 [11] J.W. Kantelhardt, *et al.*, *Phys. Rev. E* **65**, 051908 (2002).
 [12] Y. Ashkenazy *et al.*, *Physica A* **316**, 662 (2002).
 [13] C.K. Peng *et al.*, *Phys. Rev. E* **49**, 1685 (1994); A. Bunde *et al.*, *Phys. Rev. Lett.* **85**, 3736 (2002).
 [14] Unlike the power spectrum, the detrended fluctuation analysis (DFA) is capable to remove polynomial trends from the data [13]. Before applying the DFA method, we filtered out the seasonal periodicity of the data.
 [15] A. Becker and P. Braun, *J. Hydrol.* **217**, 239 (1999).